# Suppressor of Fused regulation of Hedgehog Signaling is Required for Proper Astrocyte Differentiation

**Danielle M. Spice [1,2], Joshua Dierolf [3] and Gregory M. Kelly [1-3,*]**

[1] Molecular Genetics Unit, Department of Biology, Western University, London, ON, Canada
[2] Children's Health Research Institute, London, ON, Canada
[3] Department of Physiology and Pharmacology, Western University, London, ON, Canada

*** Correspondence:**
Gregory M. Kelly
gkelly@uwo.ca

**Keywords: suppressor of fused[1], hedgehog[2], astrocyte[3], neuron[4], signaling[5], differentiation[6], CRISPR-Cas9[7].**

## Abstract

Hedgehog signaling is essential for vertebrate development, however, less is known about the negative regulators that influence this pathway during the differentiation of cell fates. Using the mouse P19 embryonal carcinoma cell model, Suppressor of Fused (SUFU), a negative regulator of the Hedgehog pathway, was investigated during retinoic acid-induced neural differentiation. We found Hedgehog signaling was activated in the early phase of neural differentiation but was inactive during terminal differentiation of neurons and astrocytes. This early activation was required for neural differentiation however, it alone was not sufficient to induce neural lineages. SUFU, which regulates signaling at the level of GLI, remained relatively unchanged during the differentiation process, but its loss through CRISPR-Cas9 gene editing resulted in ectopic expression of Hedgehog target genes. Interestingly, these SUFU-deficient cells were unable to differentiate in the absence of retinoic acid, but when differentiated using retinoic acid, they showed delayed and decreased astrocyte differentiation; neuron differentiation was unaffected. Ectopic activation of Hh target genes in SUFU-deficient cells remained throughout retinoic acid-induced differentiation and this phenotype was accompanied by the loss of GLI3, despite the presence of the *Gli3* message. Thus, the study indicates the proper timing and proportion of astrocyte differentiation requires SUFU, and its normal regulation of GLI3 to maintain Hh signaling in an inactive state.

## 1 Introduction

Hedgehog (Hh) signaling plays pivotal roles in vertebrate development, and its deregulation leads to birth defects and/or cancer progression. In normal neural development Sonic Hedgehog (SHH) is essential in patterning the differentiation of motor neurons and interneurons in the developing neural tube [1] and it induces the differentiation of cerebellar neurons and glial cells [2]. When canonical signaling is off and the Hh ligand is absent, the transmembrane receptor Patched (PTCH) inhibits the transmembrane protein Smoothened (SMO) from translocating to the plasma membrane of the primary cilium [3]. This inhibition allows the scaffolding protein Suppressor of Fused (SUFU) to sequester full length GLI transcription factors in the cytoplasm [4] or promotes GLI phosphorylation [5] and subsequent partial proteosomal degradation into a truncated repressor [6,7]. In the presence of Hh, however, PTCH is bound and relieves the inhibition of SMO. This allows the SUFU-GLI complex to be recruited into the primary cilium [8] where SUFU dissociates from GLI

allowing the translocation of GLI to the nucleus where it acts as a transcriptional activator [7]. In vertebrates there are three GLI transcription factors, GLI1, GLI2 and GLI3. GLI1 acts solely as an activator, and as a Hh target gene is present only after activation of Hh signaling [6]. GLI3 acts primarily as a transcriptional repressor, although both GLI2 and GLI3 can act as either activators or repressors [6]. Thus, while Hh target gene transcription is tightly regulated through GLI, the GLI's are also regulated by other proteins.

SUFU plays an essential role in regulating GLI processing, and thus is key to Hh pathway activation. *Sufu* loss of function alleles result in the constitutive expression of Hh target genes in the absence of a Hh ligand [9,10], through the reduced processing and stability of the GLI3 repressor [11]. Activation of Hh signaling through *Sufu* loss in humans causes medulloblastoma tumor growth [12,13] and Nevoid Basal Cell Carcinoma Syndrome [13,14], while mouse embryos containing a targeted deletion of *Sufu* are embryonic lethal at E9.5 due to neural tube closure defects [10]. Furthermore, the specific loss of *Sufu* function in the cerebellum results in developmental delays in neuron differentiation [15] and cerebellum mispatterning [16].

In the present study an *in vitro* system utilizing the mouse P19 embryonal carcinoma cell line was employed to study when the Hedgehog pathway is activated, the requirement of Hh during differentiation and the effects of *Sufu* loss of function on neural cell fate. The cell line, derived from the resulting teratoma of the subcutaneous implantation of a E7.5 mouse embryo into the testis of another mouse [as reviewed in 17] are readily differentiated into neural lineages in the presence of retinoic acid (RA) [18]. RA-induced differentiation of P19 cells forms functional neurons and supporting astrocytes [19], and although this is well-known, few studies have investigated the role of Hh signaling in this system [20,21]. Of these, the role of *Gli2* was reported, but where one study shows the overexpression of a constitutively active *Gli2* promotes neuronal differentiation [20], another reveals the knockdown of *Gli2* causes the same phenotype [21]. Even though Hh signaling is precisely controlled in neural cell fate decisions *in vivo,* and that this is mediated through negative regulators, what remains to be determined is how SUFU is involved in determining neuron and astrocyte cell fate decisions. To address this shortfall, this study aims to better understand the essential role of SUFU in neuroectodermal differentiation. Using the P19 cell model and timeline investigations, we show when Hh signaling is activated and required during RA-induced neural differentiation, and through genetic ablation of *Sufu,* demonstrate that there is an essential role for it, specifically, in astrocyte fate determination.

## 2 Materials & Methods

### 2.1 Cell culture & Differentiation

P19 embryonal carcinoma cells (a gift from Dr. Lisa Hoffman, Lawson Health Research Institute, London, ON, Canada) and *Sufu* knockout (*Sufu*$^{-/-}$, described below) P19 cells were cultured on adherent tissue culture plates in DMEM containing 5% fetal bovine serum (FBS) and 1% pen/strep at 37°C and 5% $CO_2$. For passaging, cells were trypsinized (TrypLE Express), centrifuged and re-suspended as single cells every 4 days or at 70% confluency, whichever occurred first. Differentiation of P19 cells was adapted from McBurney et al. 1988 [19]. To induce neural differentiation, approximately $1.05 \times 10^6$ cells were cultured on bacterial grade Petri dishes for 4 days in 0.5 µM RA to form embryoid bodies. After this incubation, aggregates were subsequently plated on adherent tissue culture dishes in the presence of 0.5 µM RA, for a total of 10, 14 or 17 days. Untreated controls were grown for 4 days on bacterial grade Petri dishes and re-plated on adherent tissue culture dishes for the total number of days stated above. For Smoothened Agonist (SAG; EMD Millipore) and Cyclopamine (Cyc, EMD Millipore) studies $1.05 \times 10^6$ cells were cultured on bacterial grade Petri dishes for 4 days in 0.5 µM RA plus 10 nM SAG or 10 µM Cyc, or 10 nM SAG alone to

form embryoid bodies; then, embryoid bodies were aggregated and subsequently re-plated in the presence of 0.5 μM RA or were left untreated for SAG-only treatment.

### 2.2 Cas9 plasmid preparation

The pSpCas9(BB)-2A-Puro (PX459) V2.0 (Addgene plasmid 62988; http://n2t/addgene:62988) was used, where sgRNAs for *Sufu* (Supplementary Table 1) were cloned into the PX459 vector using the protocol of Ran et al. 2013 [22]. Briefly, sgRNAs were amplified and phosphorylated, the vector digested using the BbsI restriction enzyme, and vector and sgRNA were incubated at room temperature for 1.5 h for ligation. Ligated plasmids were transformed into competent DH5alpha bacteria and grown on ampicillin containing agar plates. Colonies were selected and isolated plasmids were sent for sequencing at the London Regional Genomics Centre (Robarts Research Institute, London, ON) using the U6 primer (Supplementary Table 1).

### 2.3 Knockout lines

P19 cells were incubated with 2 μg of PX459-sgRNA plasmid in 10 μL of Lipofectamine 2000 (Invitrogen). Media was changed after 4 h, and cells were grown to 70% confluency and then passaged as single cells in a 96 well plate and incubated with 1 μg/mL puromycin. Media containing 1 μg/mL puromycin was replaced every 24 h for 4 days, and then cells were grown in complete media without puromycin until ready to be passaged. Knockout genotypes were determined by collecting genomic DNA (Qiagen DNeasy® Blood & Tissue kit, 69504), and performing standard PCR (DreamTaq Master Mix (2X), Thermo Scientific, K1081) with *Sufu*-specific primers (Supplementary Table 1) and a Vapo.protect Thermocycler (Eppendorf). Amplicons were sequenced at the London Regional Genomics Centre and compared to wildtype sequences using pair-wise sequence alignment (Geneious 2021™). KO line #2 sequencing was examined using TIDE analysis (http://shinyapps.datacurators.nl/tide/) [23] to further investigate the nature of the allele. TIDE analysis was unable to interrogate KO line #1 as the length of deletion was outside of the tool parameters.

### 2.4 Overexpression lines

The P19 cell line with the 1 bp insertion into the *Sufu* gene (KO #2) was transfected with either 1436 pcDNA3 Flag HA (Addgene plasmid # 10792 ; http://n2t.net/addgene:10792 ; RRID:Addgene_10792); a pcDNA Flag HA vector with the *Sufu* open reading frame cloned from the pcDNA Su(fu) (CT #116) (Addgene plasmid # 13857 ; http://n2t.net/addgene:13857 ; RRID:Addgene_13857)[24] using BamHI (R0136, New England Biolabs) and XhoI (R0146, New England Biolabs) restriction enzymes; or hGli3 flag3x (Addgene plasmid # 84921 ; http://n2t.net/addgene:84921 ; RRID:Addgene_84921) using Lipofecatime 2000 (Invitrogen). Cells were incubated for 4 hours in the presence of plasmid, where media was then changed, and cells were grown to 70% confluency. Transfected cells were passaged, incubated for 24 hours, then treated with 500 μg/mL neomycin (G418, BioShop) selection media. Every 48 hours selection media was replaced for a total of 2 weeks.

### 2.5 Real-time reverse transcriptase PCR

To determine relative mRNA expression levels total RNA was collected from differentiated P19 cells after 1, 2, 3, 4, 6, 8, 10, 14 and 17 days after initial treatment (where cells collected between days 1-4 were in aggregates and those collected between days 6-17 were re-plated cells) using QiaShredder (Qiagen, 79654) and RNeasy (Qiagen, 74104) kits. RNA was reverse transcribed into

cDNA using a High-Capacity cDNA Reverse Transcription Kit (Thermo Fisher Scientific, 4368814). Primers were designed for: *L14*, *Shh*, *Ihh*, *Dhh*, *Smo*, *Ptch1*, *Ptch2*, *Sufu*, *Gli1, Gli2, Gli3*, *Ascl1*, *NeuroD1*, *NeuroG1* and Chicken *Sufu* (Supplementary Table 1). RT-qPCR was conducted according to the following reaction conditions: 500 nM of each reverse and forward primers, 10 µL of SensiFAST SYBR No-ROX Mix (Bioline, FroggaBio, BIO-98050), and 1 µL of cDNA template. Samples were analyzed using a CFX Connect Real-Time PCR Detection System (Bio-Rad) using the comparative cycle threshold method ($2^{-\Delta\Delta Ct}$). Relative mRNA expression was normalized to *L14* expression and were subsequently normalized to untreated or wildtype untreated controls to determine fold change expression.

## 2.6 Immunoblot Analysis

Cells were lysed in 150-500 µL of 2% sodium dodecyl sulfate buffer containing 62.5 mM Tris-HCL pH 6.8, 10% glycerol, 5% mercapto-2-ethanol and 1X Halt Protease Inhibitor Cocktail (Thermo Scientific, 1862209) at a 1:200 ratio. Protein lysates were sonicated for 30 sec on ice and protein concentrations were measured using the DC™ Protein Assay (Bio-Rad, 5000113). Approximately 10-20 µg of protein were separated on denaturing 6-10% polyacrylamide gels for approximately 90 min at 120V, then transferred to PVDF membranes (Bio-Rad, 1620177) at 20V overnight at 4°C. Membranes were incubated for 1 h at room temperature in Tris-buffered saline with 0.1% Tween-20 (TBS-T) containing 5% skim milk, and then probed with primary antibodies to β-III-tubulin (TUJ1, 1:1000; Cell Signaling Technology, 5568), GLI3 (1:1000; R&D Systems, AF3690), SUFU (1:1000; abcam, ab28083), GFAP (1:1000; Invitrogen, 14-9892-80) and β-actin (1:10,000; Santa Cruz Biotechnology, sc-47778) overnight at 4°C. Membranes were washed 3 times for 5 min with 1X TBS-T and were probed with the appropriate HRP-conjugated secondary antibodies (1:10,000, Sigma) for 2 h at room temperature. After washing 3 times for 5 min with 1X TBS-T, signals were detected using the Immobilon® Classico Western HRP Substrate (Millipore, WBLUC0500) and were imaged using a Chemi Doc Touch System (Bio-Rad).

## 2.7 Immunofluorescence

P19 wildtype and *Sufu*$^{-/-}$ cells were differentiated as stated previously, on coverslips coated with poly-L-lysine hydrobromide (Sigma, P5899). Coverslips were washed 3 times with PBS before they were used for cell culture. After differentiation, cells were washed for 1 min with PBS before fixation with 4% paraformaldehyde in PBS for 10 min at room temperature. Cells were washed 3 times for 5 min with ice-cold PBS before being permeabilized in 0.2% Triton-X-100 in PBS for 10 min at room temperature, then washed 3 times for 5 min before blocking for 30 min at room temperature in 1% Bovine Serum Albumin, 22.52 mg/mL glycine and 0.1% Tween-20 in PBS. Coverslips were incubated overnight in a humidity chamber with β-III-tubulin (TUJ1, 1:400; Cell Signaling Technology, 5568) and GFAP (1:500; Invitrogen, 14-9892-80) in blocking solution. Coverslips were then washed 3 times for 5 min with PBS before cells were incubated in secondary antibodies, Alexa Fluor™ 660 goat anti-mouse IgG (Invitrogen, A21054) and Goat anti-Rabbit IgG Alexa Fluor Plus 488 (Invitrogen, A32731TR) in blocking solution in the dark for 1 h at room temperature. Coverslips were washed 3 times for 5 min with PBS in dark conditions before being mounted onto microscope slides using Slowfade™ Gold antifade reagent with DAPI (Invitrogen, S36942). Coverslips were sealed to slides using nail polish then imaged using a Zeiss AxioImager Z1 Compound Fluorescence Microscope. All immunofluorescence images were taken at the Integrated Microscopy Facility, Biotron (Western University, London, ON, Canada) and were analyzed for DAPI, β-III-tubulin and GFAP positive cells using ImageJ.

## 2.8 Flow Cytometry

P19 wildtype and *Sufu*$^{-/-}$ cells were differentiated as stated previously. Cells were washed three times with ice cold PBS wihout magnesium or chloride (PBS(-/-)) (Thermo Fisher A1286301) and dissociated with 0.25% Trypsin. Subsequent PBS(-/-) washes were completed 3 times, 5 minutes each. Trypsin was deactivated with DMEM/F12 (ThermoFisher 11320033) containing 10% ES-grade Fetal Bovin Serum (FBS) (Thermo Fisher 10439016), and then cells were centrifuged at 300 g for 5 minutes and reconstituted in PBS(-/-). Cells were counted using a trypan blue assay, separated to approximately 1.0x10$^6$ cells per tube, washed in Flow Cytometry Staining Buffer (FCSB(10% FBS in PBS(-/-)),-centrifuged as previously described and the buffer aspirated. Cells were fixed using 4% formaldehyde (Electron Microscopy Sciences 15680) in PBS(-/-) for 10 min at room temperature, washed with ice cold PBS and then permeabilized with 0.2% Triton-X-100 in PBS(-/-) for 10 min at room temperature before subsequently washing with PBS(-/-). Cells were incubated with or without 1 µL of GFAP Monoclonal Antibody (GA5), Alexa Fluor 488, eBioscience™ (Invitrogen, 53-9892-82) per million cells for 1 h at room temperature, and then washed with PBS (-/-), strained using a 40 µm cell strainer (Falcon™ C352340) and analyzed using a BD FACSCanto II flow cytometer at the London Regional Flow Cytometry Facility (Robarts Research Institute). Data were analyzed using FlowJo (BD).

## 3 Results

### 3.1 Retinoic acid and cell aggregation induces P19 neural differentiation

Neural differentiation was induced by culturing cells for 4 days in the presence of 0.5 µM RA to form cell aggregates that were then plated for an additional 6 days to form neurons or an additional 13 days to form astrocytes (Figure 1A). RT-qPCR was used to test for neural differentiation, and as expected *NeuroG1* showed increased expression between days 0-6 with a subsequent decline on days 8-10 (Figure 1B). *NeuroD1* and *Ascl1* both increased in expression throughout RA treatment to days 6-10 when neurons are forming (Figure 1C and D, respectively). Neuronal differentiation in the presence of RA was confirmed through immunoblot analysis of β-III-tubulin, a neuronal marker. As expected based on previous reports [25], β-III-tubulin was only detected following RA treatment after 10 days, and subsequently declined by 17 days (Figure 1E). Astrocyte differentiation was also confirmed through immunoblotting where Glial Fibrillary Acid Protein (GFAP), an astrocyte marker, was only detected following RA treatment, with signals increasing in abundance by day 17 (Figure 1E). Neither GFAP nor β-III-tubulin was detected in the absence of RA although cells were undergoing spontaneous differentiation through embryoid body formation (Figure 1E). Together, these results confirmed that our differentiation protocol was successful in differentiating both neurons and astrocytes in the presence of RA.

### 3.2 Hh signaling is activated early in neural differentiation

Since numerous reports have shown that Shh signaling is vital in vertebrate neural differentiation [1–3], Hh expression must be present during RA-induced P19 cell neural differentiation. RT-qPCR was used to explore Hh component expression throughout days 0-10 of RA treatment. Hh ligands *Dhh*, *Ihh*, and *Shh* (Figure 2A-C, respectively) were expressed after 1 day of RA treatment, as was the Hh target gene *Gli1* (Figure 2D). Expression of Hh pathway components *Ptch1, Ptch2, Smo, Gli2, Gli3* (Supplemental Figure 1), and *Sufu* (Supplemental Figure 3A) was also confirmed during days 0-10 of RA treatment. The presence and activity of GLI transcription factors are necessary for Hh signal activation [3], where GLI3 is key for early signal modulation, serving as either an activator or repressor [6]. Thus, the ratio between GLI3 full-length (GLI3FL) and GLI3

repressor (GLI3R) protein is an important indicator of how GLI3 is acting in the Hh pathway. Although Hh signaling was active after RA induction, it was unknown if this increase in Hh activity was due to the RA or to the embryoid body culture system. When GLI3 was examined, results showed an increase in the GLI3FL to GLI3R ratio in untreated cells (cells undergoing the embryoid body formation and replating steps but in the absence of RA), and RA-treated cells after 1 day in culture (Figure 2E and F), where in RA treated cells the repressor form of the protein subsequently

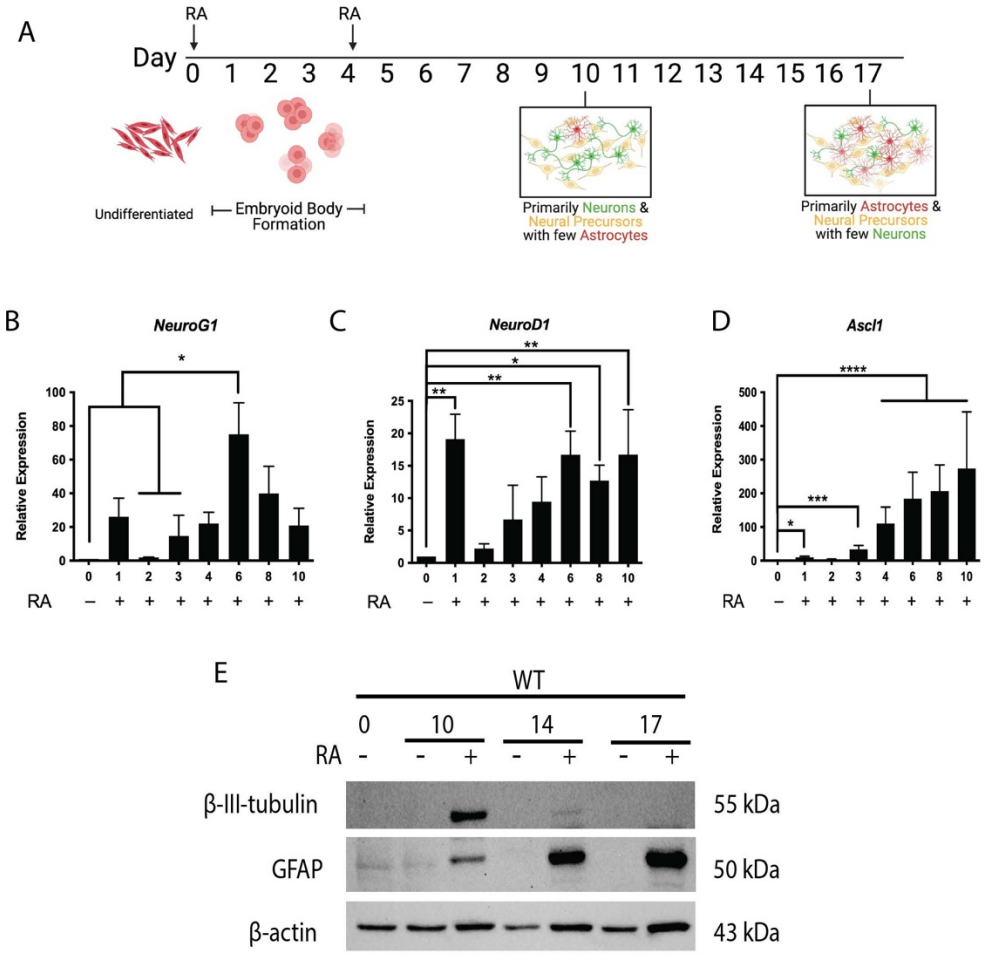


**Figure 1 – Retinoic acid is required for P19 cell neural differentiation. (A)** Schematic of *in vitro* differentiation of P19 cells toward neural lineages. **(B)** *NeuroG1,* **(C)** *NeuroD1*, and **(D)** *Ascl1* expression on days 0-10 of RA-induced differentiation. **(E)** Immunoblot of neuron marker β-III-tubulin and astrocyte marker GFAP on days 0-17 of RA-induced differentiation. N=3. Bars represent mean values ± s.e.m. *$^*P<0.05$, $^{**}P<0.01$, $^{***}P<0.001$, $^{****}P<0.0001$*. Panel A was created using BioRender.com.

increases in abundance from days 2-10 (Figure 2E). The significant increase in the GLI3FL to GLI3R ratio in untreated cells was unexpected, as these cells, undergoing spontaneous differentiation, do not differentiate into either neurons or astrocytes (Figure 1E). This result suggests that the three-dimensional culture system of embryoid body formation is key to the activation of Hh signaling seen in the RA-treated cells. Exploring later time points associated with astrocyte differentiation (days 10-17), the GLI3FL to GLI3R ratio in RA treated cells was not significantly different from untreated controls (Figure 2G). Given these data it would appear the Hh pathway is activated early in the neural differentiation of these cells, due to the formation of embryoid bodies, leading to GLI3 activation, but

this early activation is quenched and remains in the off state for the remainder of RA-induced differentiation.

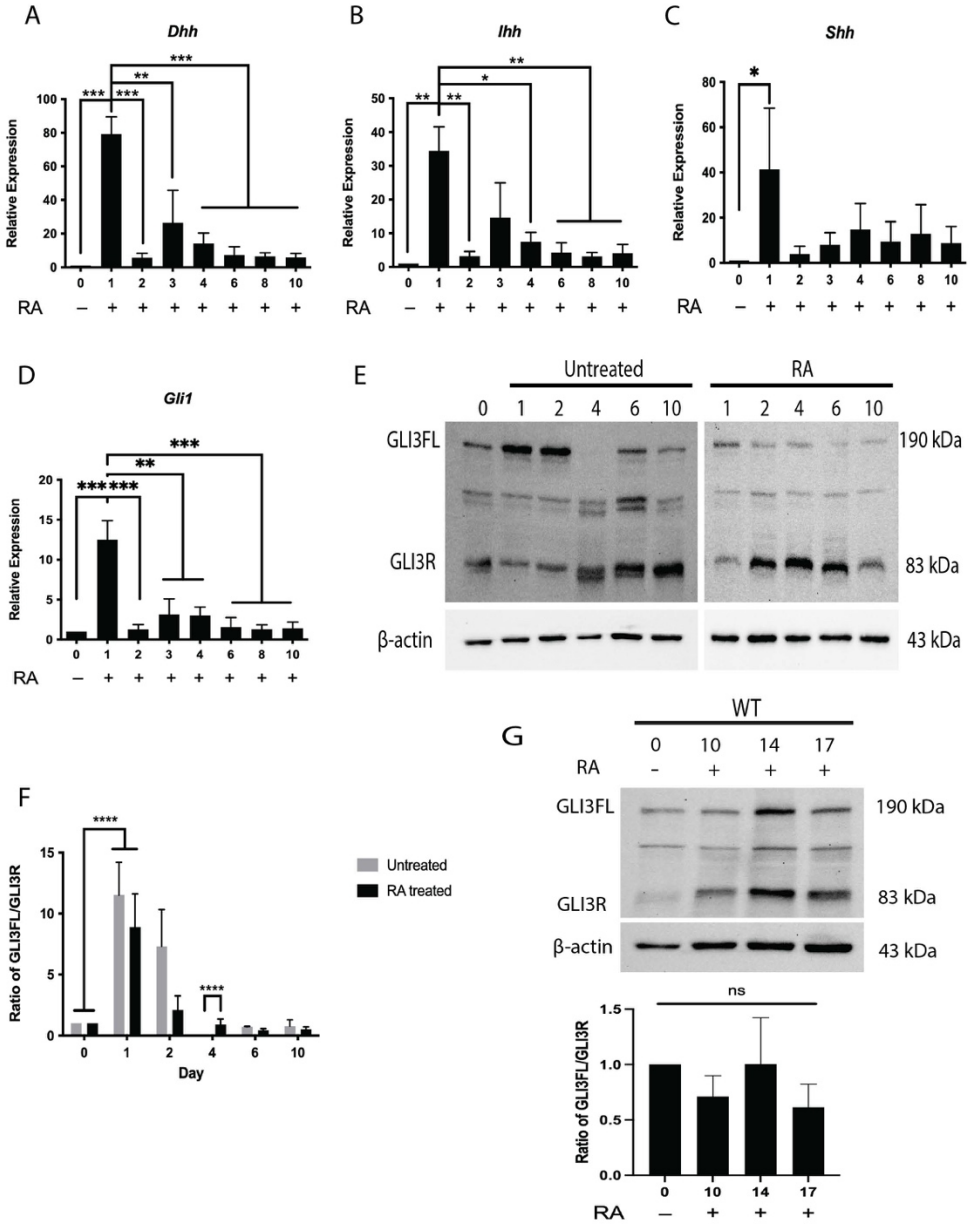


**Figure 2 – Hh signaling is activated early in RA-induced differentiation.** RT-qPCR showing expression of Hh ligands **(A)** *Dhh*, **(B)** *Ihh*, and **(C)** *Shh*, and Hh target gene **(D)** *Gli1* on days 0-10 of RA-induced differentiation. **(E)** Immunoblot of GLI3 full length (GLI3FL) and GLI3 repressor (GLI3R) on days 0-10 of untreated or RA-induced cells. **(F)** Densitometric analysis of GLI3FL to GLI3R ratio from previous immunoblot**.** (**G)** Upper panel: Immunoblot of GLI3FL and GLI3 repressor on days 0-17 of RA-induced cells, lower panel: densitometric analysis of upper panel. N=3. Bars represent mean values ± s.e.m. *$^*P<0.05$, $^{**}P<0.01$, $^{***}P<0.001$, $^{****}P<0.0001$.*

## 3.3 Early Hh signaling is required but not sufficient for neural differentiation

As Hh signaling is activated early in P19 neural differentiation (Figure 2 and Supplemental Figure 1), we sought to determine if activation or attenuation of this pathway would affect

differentiation. To address this, cells were treated with either Hh pathway activator, Smoothened Agonist (SAG) or inhibitor, Cyclopamine (Cyc) (Figure 3). Following the paradigm outlined in Figure 1A, cells were treated with 0.5 μM RA (RA), 0.5 μM RA plus 10 nM SAG (RA + SAG), 10 nM SAG alone with no subsequent RA treatment on day 4 (SAG) or 10 nM SAG on day 0 with subsequent 0.5 μM RA treatment on day 4 (SAG + RA). Immunoblot analysis showed the neuron marker, β-III-tubulin in the RA, RA + SAG and SAG + RA treatments but not in the SAG treatment alone on day 10 (Figure 3A). Densitometric analysis revealed an increase in β-III-tubulin intensity in the RA + SAG treatment compared to RA alone at day 10, but no difference between RA alone and the SAG + RA treatment at day 10 (Figure 3A). Experiments allowing cell aggregation for 4 days in the absence of RA, then subsequent 0.5 μM RA treatment at day 4 (Untr + RA), also showed a β-III-tubulin signal at day 10, however this signal was less than the RA treatment alone on the same day (Supplemental Figure 2A and B). Together, this data suggests that early activation of Hh signaling, with SAG, is not sufficient to induce neuron differentiation, however, additional cues provided by subsequent RA treatment is sufficient to induce the neuron lineage (Figure 3A). This data also shows that the over-activation of Hh with SAG can enhance the neuron cell fate.

Immunoblot analysis of the astrocyte marker GFAP showed detection on day 17 in the RA and RA + SAG treatments, but no detection in the SAG alone (Figure 3A). Densitometric analysis showed increased GFAP intensity in the RA + SAG treatment compared to RA treatment alone (Figure 3C). There was an apparent band in the SAG + RA treatment (Figure 3A), but densitometric analysis revealed that this signal was not significantly different from the SAG alone treatment (Figure 3C). Untr + RA treated cells, also showed this low level of GFAP at day 17 (Supplemental Figure 2A and C), indicating that RA treatment at this later time was sufficient to induce astrocytes, however not to the extent observed with the initial RA treatment. Thus, it appears from immunoblot data that supplementing the initial RA treatment with SAG increases astrocyte differentiation, while treatment with SAG followed by RA (Figure 3A) or aggregation alone and then RA treatment (Supplemental Figure 2A) induces low levels of astrocyte differentiation. In addition, activation of Hh signaling alone using SAG was insufficient to induce the astrocyte fate. Together, these results would indicate that activation of Hh through SAG treatment alone is not sufficient to induce these neural lineages, however, SAG treatment in the presence of RA does enhance differentiation of both neurons and astrocytes.

Since early Hh pathway activation enhances neural cell fates, but activation of the pathway alone using SAG is insufficient, we were then interested in determining if neural cell fate would be altered if Hh signaling was attenuated with Cyc. Again, following the paradigm outlined in Figure 1A cells were treated with either 0.5 μM RA (RA) or 0.5 μM RA plus 10 μM Cyc on day 0 (RA + Cyc); both with subsequent RA treatments on day 4. Immunoblot analysis to detect β-III-tubulin on day 10 showed signals in both RA and RA + Cyc treatments (Figure 3D), however densitometry revealed the intensity was significantly reduced in the Cyc treatment (Figure 3E). GFAP levels were eliminated by Cyc, regardless of the presence of RA (Figure 3D, quantified in Figure 3F). Experiments with cells treated with RA plus the Cyc vehicle (DMSO) showed no significant change in either marker (Supplemental Figure 2D-F). These results would indicate that specific inhibition of the Hh pathway attenuates both neuron and astrocyte cell fates, and thus is required for proper differentiation of these cell types.

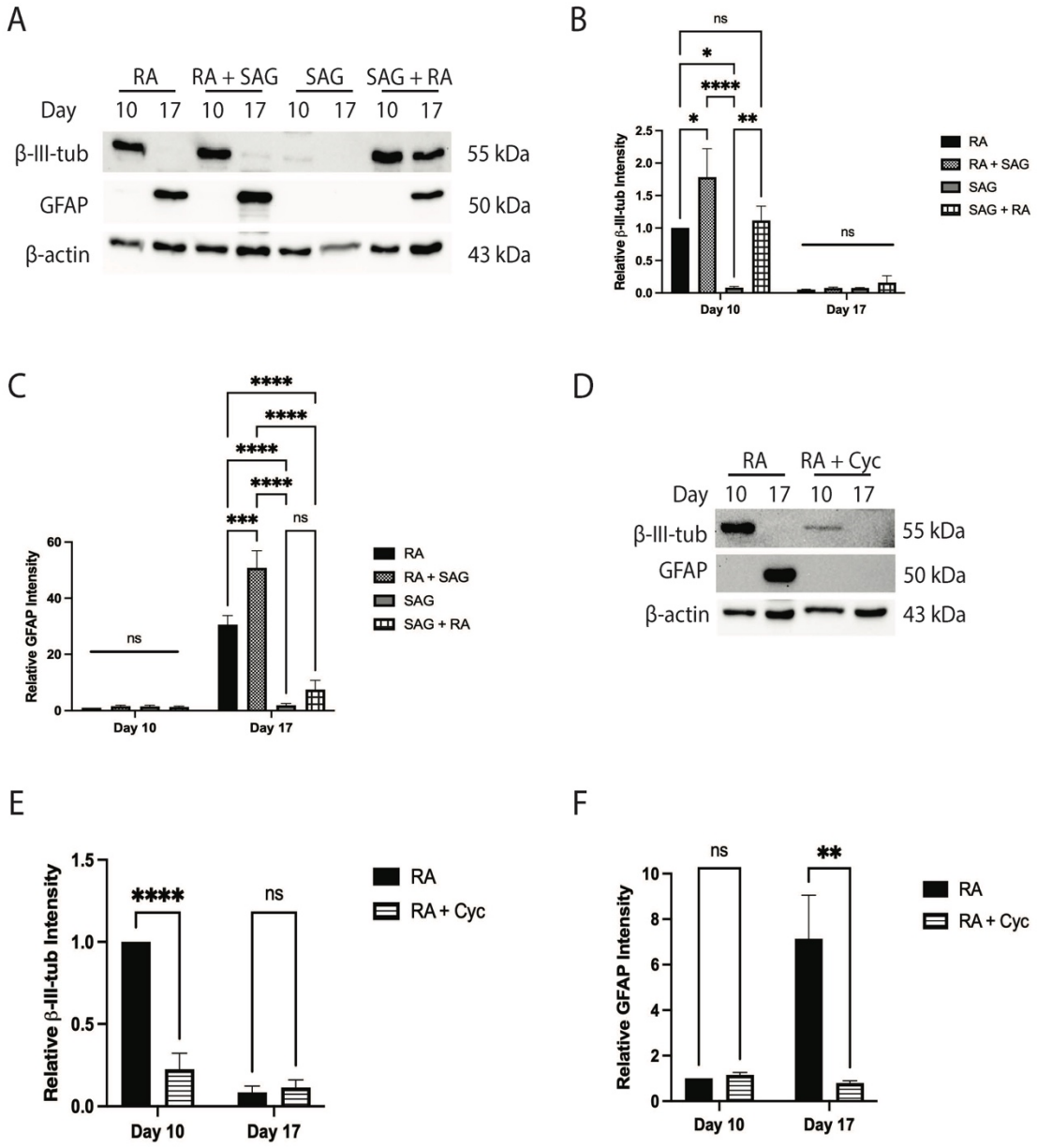


**Figure 3 – Early Hh pathway activation is required but not sufficient to induce neural lineages. (A)** Immunoblot of neuron marker β-III-tubulin and astrocyte marker GFAP on days 10 and 17 of cells induced to differentiate in the presence of RA alone, RA plus SAG, SAG alone or SAG plus subsequent RA treatment. **(B)** Densitometry of β-III-tubulin and **(C)** of GFAP from immunoblot in A. **(D)** Immunoblot of β-III-tubulin and GFAP on days 10 and 17 of cells induced to differentiation in the presence of RA alone or RA plus Cyc. **(E)** Densitometry of β-III-tubulin and **(F)** GFAP from immunoblot in D. N=3. Bars represent mean values ± s.e.m. **P<0.05, **P<0.01, ***P<0.001, ****P<0.0001*.

### 3.4 SUFU levels during neural differentiation

Given that Hh signaling is induced early, and early activation of this pathway is required for neural differentiation, we were next interested in understanding the role negative regulators have on neuron and astrocyte formation. One gene of interest, *Sufu,* encodes a negative regulator of the pathway that inhibits GLI activity and as reported by Humke et al. [7], promotes GLI3 conversion to a repressor. During neural differentiation, relative to day 0, *Sufu* gene expression increased on day 1,

8 and 10 of RA treatment (Supplemental Figure 3A); however, at the protein level no significant changes were observed in SUFU levels between untreated and RA treated cells (Supplemental Figure 3B; densitometric analysis in Supplemental Figure 3C). Similarly, *Sufu* expression on days 10-17 showed no significant change relative to the control on day 0 (Supplemental Figure 3D); however, SUFU protein intensity decreased at these later stages (Supplemental Figure 3E and F). Given that *Sufu* expression remains largely unchanged and only at later stages, coinciding with astrocyte differentiation, do protein levels decrease, it is tempting to speculate that the early activation of the Hh pathway is controlled by the cellular localization or post-translational modification status of SUFU.

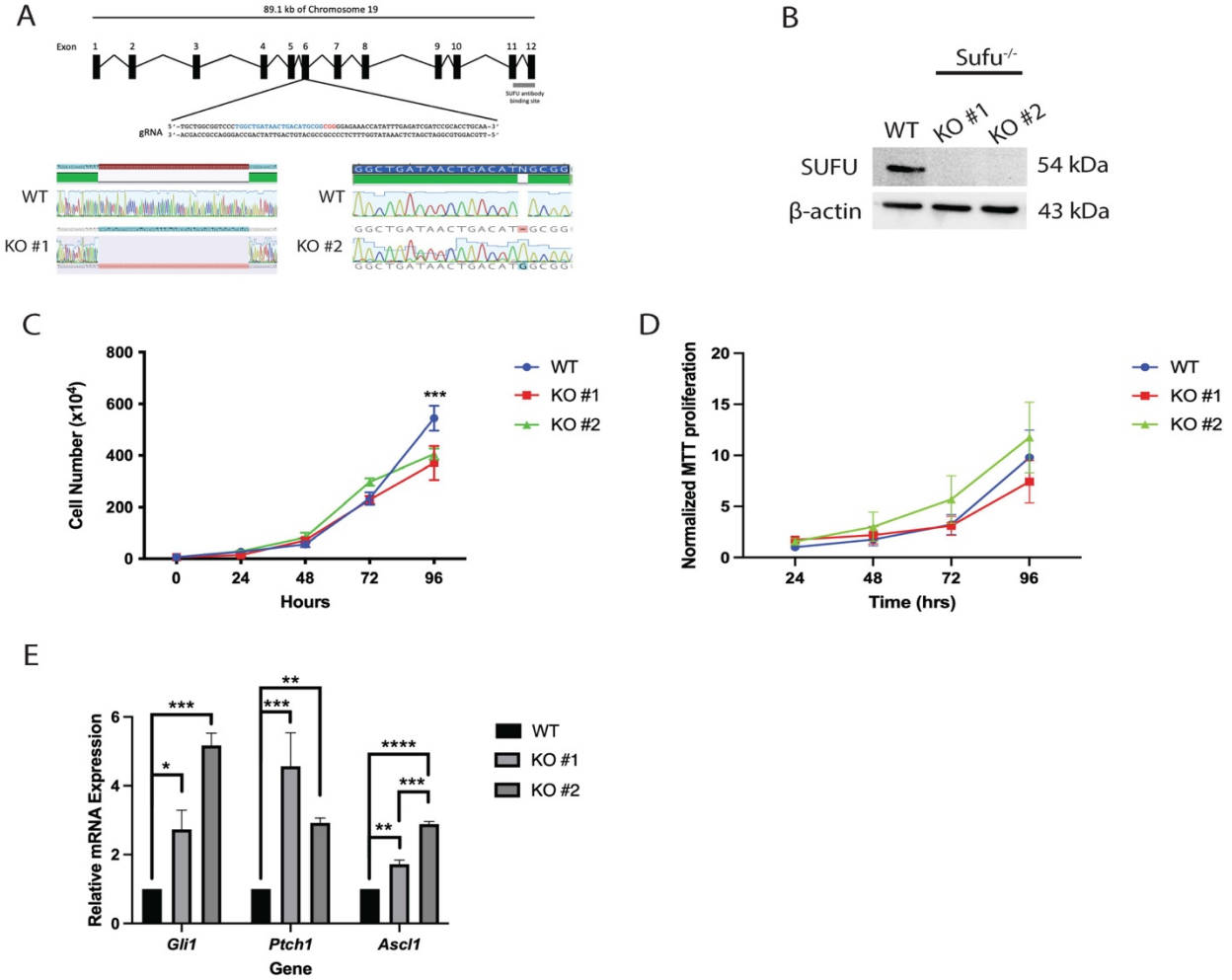


**Figure 4 – CRISPR-Cas9 knock out of *Sufu* activates Hh signaling in undifferentiated P19 cells. (A)** Schematic showing gRNA targeting exon 6 of the *Sufu* gene yielding two KO clones. **(B)** Immunoblot of SUFU levels in wildtype (WT) and *Sufu*$^{-/-}$ clones. **(C)** Cell count curves of WT and *Sufu*$^{-/-}$ clones between 0-96 hours and **(D)** MTT assay normalized to WT cells at 24 hrs. **(E)** Expression of Hh target genes *Gli1*, *Ptch1* and *Ascl1* in WT and *Sufu*$^{-/-}$ clones on day 3 of undifferentiated cultures. N=3. Bars represent mean values ± s.e.m. **P<0.05, **P<0.01, ***P<0.001, ****P<0.0001.*

## 3.5 Sufu knockout activates Hedgehog signaling

Aberrant SUFU activity is associated with tumorigenesis [12–14], and given that SUFU acts as an essential regulator of GLI3 [7], and GLI2 [4,7] and from data above, its loss was expected to induce Hh signaling. To test this, CRISPR-Cas9 was used to target exon 6 of the *Sufu* gene (Figure

4A). Gene targeting resulted in the formation of two clones, one with an 81 bp deletion (KO #1) that spans the intron-exon boundary between intron 5 and exon 6 and another with a 1 bp insertion (KO #2). *In silico* analysis was performed for the predicted translation of the 81 bp deletion (KO #1) and it revealed a premature stop codon at amino acid location 231 of the 484 amino acid SUFU polypeptide. The second mutation, KO #2, revealed by sequence alignment and TIDE analysis [23] showed a 1 bp insertion of a guanine residue just upstream of the PAM sequence, also resulting in a premature stop codon at amino acid location 246 of the polypeptide (Supplemental Figure 4). Immunoblot analyses using a SUFU antibody targeted to the C-terminal end of the polypeptide, a region previously reported to be required for GLI binding [4,26], showed a signal in WT cells after 3 days in untreated monolayer culture; however, no signal was detected in either mutant under the same culture conditions (Figure 4B).

CRISPR-Cas9-generated mutant *Sufu*$^{-/-}$ alleles resulted in decreased cell numbers compared to WT cells cultured to 96 h (Figure 4C); however, additional MTT analysis at the same timepoints show no change in relative MTT absorbance (Figure 4D). Furthermore, compared to WT cells, KO *Sufu* lines #1 and #2 showed significantly increased Hh target *Gli1*, *Ptch1*, and *Ascl1* expression in undifferentiated, monolayer cultures (Figure 4E). Together, the data show the loss of SUFU does not greatly affect the proliferation of undifferentiated cells, but loss of SUFU aberrantly induces the activation of transcriptional targets of the Hh pathway in untreated cells.

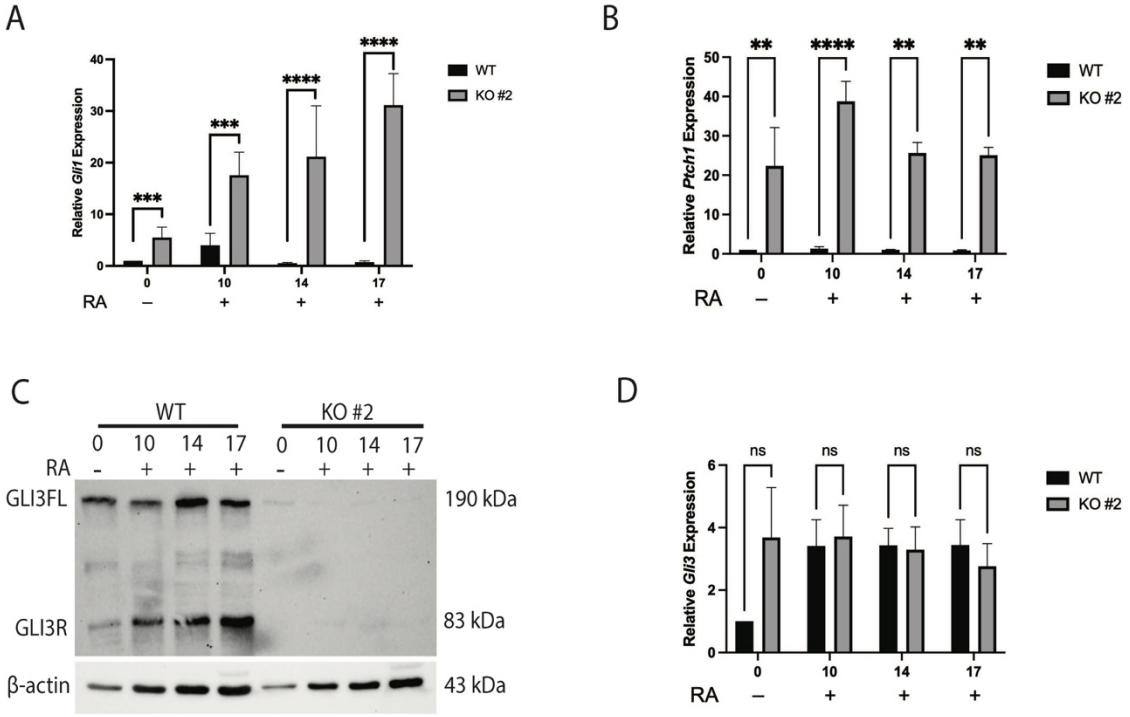


**Figure 5 –*Sufu*$^{-/-}$ maintains activate Hh signaling and causes the loss of Gli3.** Expression of Hh target genes **(A)** *Gli1* and **(B)** *Ptch1* and **(C)** *Gli3* encoding transcription factor in wildtype (WT) and *Sufu*$^{-/-}$ KO #2 cells on days 0-17. **(D)** Immunoblot of GLI3 full length (GLI3FL) and GLI3 repressor (GLI3R) in WT and *Sufu*$^{-/-}$ KO #2 cells on days 0-17. N=3. Bars represent mean values ± s.e.m. **P<0.05, **P<0.01, ***P<0.001, ****P<0.0001*.

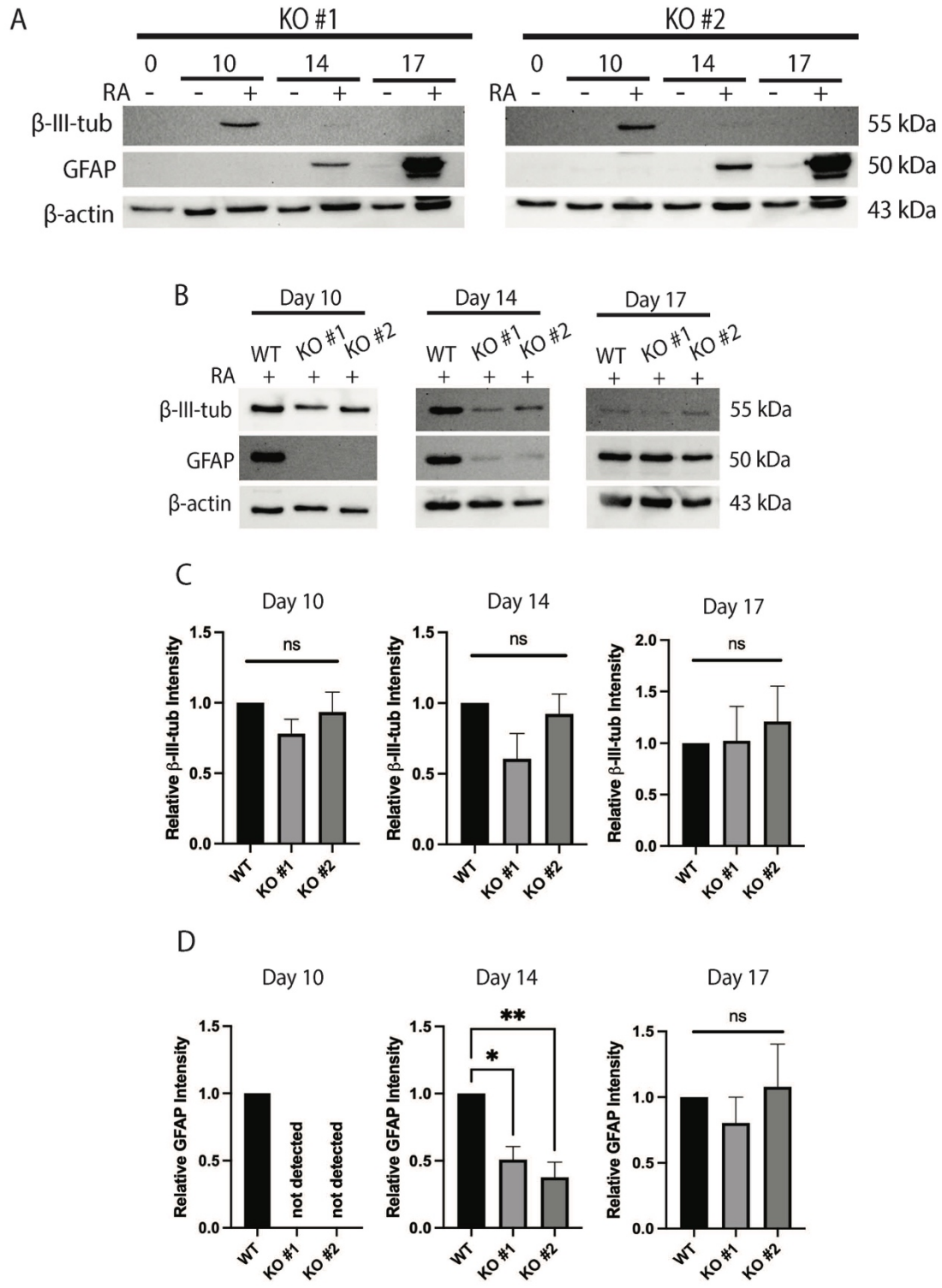


**Figure 6 – *Sufu*$^{-/-}$ delays astrocyte formation without affecting neuron differentiation. (A)** Immunoblot of neuron marker β-III-tubulin and astrocyte marker glial fibrillary acidic protein (GFAP) on days 0-17 in *Sufu*$^{-/-}$ KO clones. **(B)** Immunoblots of β-III-tubulin and GFAP on day 10, day 14 and day 17 in wildtype (WT) and *Sufu*$^{-/-}$ clones, and densitometric analyses of immunoblots of B) showing relative intensities of **(C)** β-III-tubulin and **(D)** GFAP. N=3. Bars represent mean values ± s.e.m. *$P<0.05$, **$P<0.01$.

### 3.6 Sufu loss activates Hh signaling through loss of Gli3

Given that we found *Sufu*$^{-/-}$ induced expression of Hh target genes in untreated, undifferentiated conditions (Figure 4E), we wanted to determine if this activation of Hh signaling was maintained throughout RA-induced neural differentiation. RT-qPCR results showed that *Sufu*$^{-/-}$ cells had significantly higher Hh target gene *Gli1* expression compared to WT cells at day 0, 10, 14 and 17 of RA treatment (Figure 5A and Supplemental Figure 5A). *Ptch1*, another Hh target gene was explored, and like the *Gli1* expression patten, it too showed significantly higher expression in *Sufu*$^{-/-}$ cells compared to WT cells treated with RA at all timepoints investigated (Figure 5B and Supplemental Figure 5B). Given previous work showing the connection between SUFU and GLI3 processing [7], we investigated *Gli3* expression and protein levels. No significant differences were seen in *Gli3* expression between *Sufu*$^{-/-}$ and WT cells in KO#2 (Figure 5C), however significantly decreased *Gli3* levels were observed at days 10, 14 and 17 in KO #1 (Supplemental Figure 5C). At the protein level, neither the GLI3 repressor nor the full-length form of the protein were detected in the *Sufu*$^{-/-}$ cells KO #2 (Figure 5D), and this was consistent with KO #1 having decreased or absent GLI3 levels (Supplemental Figure 5D). Thus, the loss of SUFU likely caused post-translational perturbations to the GLI3 protein causing its loss, and the observed higher expression of Hh target genes.

### 3.7 Sufu knockout delays and decreases the astrocyte cell fate

Given that *Sufu*$^{-/-}$ cells have ectopic Hh target gene expression (Figure 4 and Figure 5) leading to loss of GLI3 (Figure 5) and that early activation of Hh signaling by SAG enhanced both neuron and astrocyte cell fates when RA was present (Figure 3), we wanted to test the effect that the *Sufu* knockout had on neural lineages. First, to confirm that the KO cells would not induce differentiation in the absence of RA, cells were aggregated and replated in the absence or presence of RA as outlined in Figure 1A. With RA, results in both KO lines showed β-III-tubulin detection at day 10 and GFAP signals on days 14 and 17; neither marker was detected in the absence of RA (Figure 6A). Confident that *Sufu*$^{-/-}$ cells were unable to induce markers of differentiation without RA, we then compared both knockout lines to WT cells at days 10, 14 and 17 in the presence of RA to determine if the timing or degree of differentiation was affected by the loss of SUFU (Figure 6B). Densitometric analyses confirmed that no significant changes were seen in β-III-tubulin levels between WT and KO cells (Figure 6C). Astrocyte differentiation was, however, affected and GFAP signals on immunoblots were absent on day 10 of RA treatment in *Sufu*$^{-/-}$ cells compared to WT cells (Figure 6B). The absence of GFAP on day 10 is interpreted cautiously, as even in WT cell differentiation there are inconsistencies in the level of GFAP detection at this time point (Figure 1E and Figure 8C). GFAP levels are however consistently high in WT cells at day 14 of RA treatment (Figure 1E, Figure 6B and Figure 8C) and were significantly reduced in the *Sufu*$^{-/-}$ lines on day 14 compared to WT cells (Figure 6B and 6D). Thus, it appears removing SUFU, a key negative regulator of the Hh pathway throughout the differentiation, had an effect and delayed astrocytes from differentiating when RA was present. This idea was tested using other means and results presented below.

Immunofluorescence analyses and antibodies to β-III-tubulin and GFAP were used on WT and *Sufu*$^{-/-}$ cells at day 17 of RA treatment to confirm immunoblots showing astrocyte differentiation was restored in *Sufu*$^{-/-}$ cells on day 17 (Figure 6D). Although expecting no differences in either marker between the two cell lines, as suggested from immunoblots and their quantification (Figure 6C and D), immunofluorescence analysis showed *Sufu*$^{-/-}$ cells appeared to have no difference in β-III-tubulin positive cells, however appeared to have fewer GFAP-positive cells (Figure 7A). Images were quantified for β-III-tubulin and GFAP confirming no change in the number of β-III-tubulin positive cells and a reduction in the number of GFAP positive cells (Figure 7A). As these cells are highly heterogenous at this time point and exist in areas of high-density, flow cytometry was also performed, and results showed WT cells having a significantly higher population (~60-70% of live

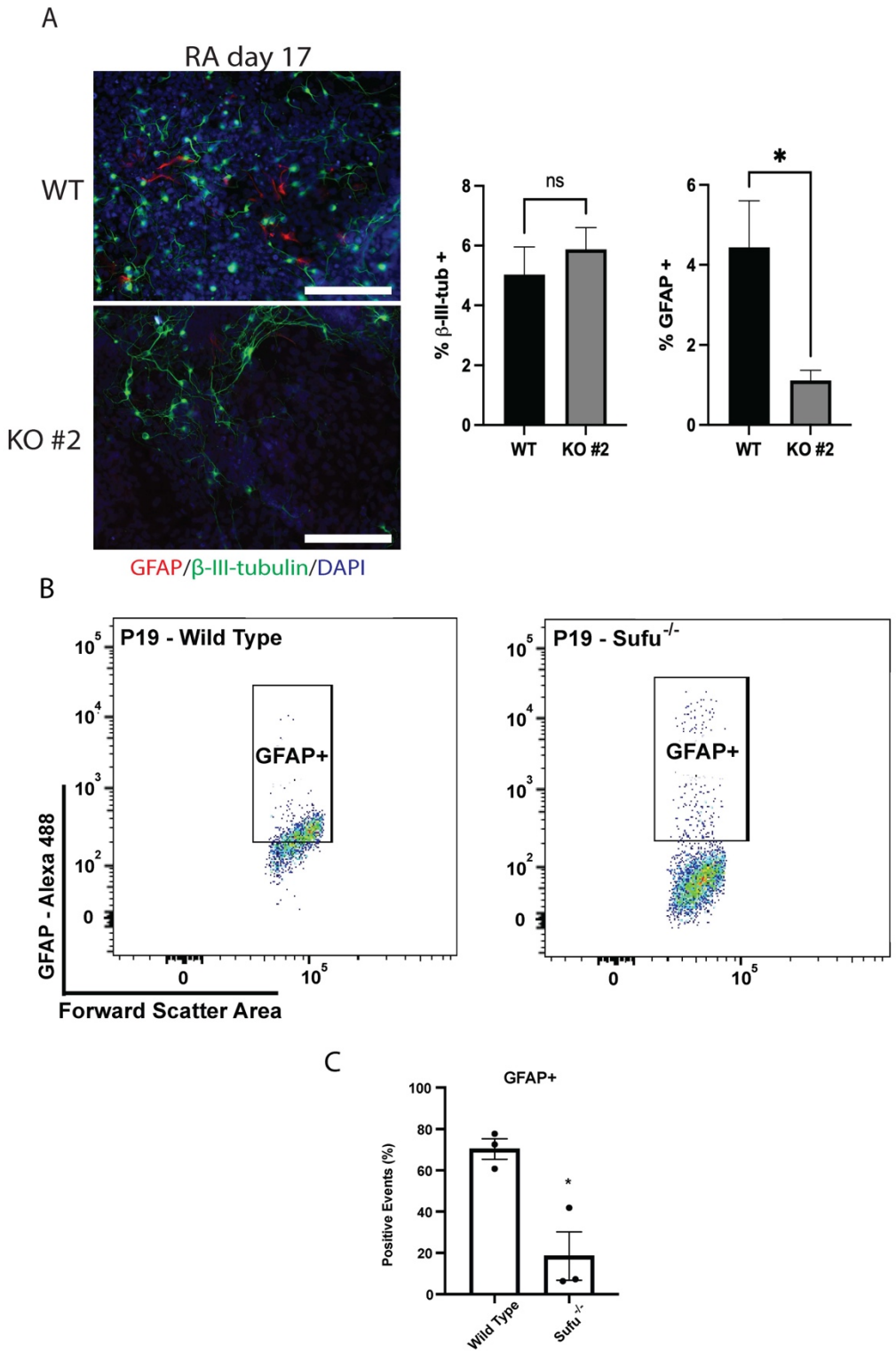


**Figure 7 - *Sufu*$^{-/-}$ decreases astrocyte differentiation. (A)** Astrocyte marker glial fibrillary acidic protein (GFAP) immunofluorescence (red), neuron marker β-III-tubulin (green) and nuclear DAPI (blue) in cells of wildtype (WT) and *Sufu*$^{-/-}$ KO clone #2 on day 17. Scale bar = 200 µm. **(B)** Flow cytometry of GFAP-positive WT and *Sufu*$^{-/-}$ KO #2 cells on day 17 and quantified in **C**. N=3. *$P<0.05$.

cells) of GFAP-positive cells compared to *Sufu*$^{-/-}$ cells (~6-25% of live cells) (Figure 7B). Statistical analysis on the flow data confirmed the immunofluorescence results and showed that there were fewer GFAP-positive cells in the *Sufu*$^{-/-}$ population (Figure 7C). Although the immunoblot data at day 17 was inconsistent with the above data, the flow cytometry identified individual cells with very high GFAP levels (Figure 7B), although overall there were fewer GFAP positive cells present in the dish. It is possible that these GFAP high cells could have been masking the decreased number of differentiated cells when the immunoblot technique was used. Together, these data support that the loss of *Sufu* does not alter neuronal differentiation, however, *Sufu* loss delayed and decreased astrocyte differentiation.

### 3.8 Sufu or Gli3 overexpression partially rescues astrocyte phenotype

We showed the loss of *Sufu* resulted in delayed and decreased astrocyte differentiation (Figure 6 and Figure 7) and results suggested that this was due to the loss of both full-length and repressor forms of GLI3 (Figure 5D and Supplemental Figure 5D). To confirm the essential roles of SUFU and GLI3 in astrocyte differentiation, we overexpressed a CRISPR-insensitive chicken *Sufu* (pSUFU) construct or human *GLI3* (pGli3) in *Sufu* knockout cells and confirmed overexpression through RT-qPCR of Chicken *Sufu* and immunoblotting of GLI3 (Supplemental Figure 6). We previously showed that *Sufu* knockout had no effect on neuron differentiation by measuring neuron marker β-III-tubulin levels (Figure 6), and this result was further confirmed in *Sufu* knockout pcDNA transfected controls at all timepoints tested (Figure 8). Surprisingly, knockout cells stably transfected with either chicken pSUFU or human pGli3 vectors had decreased β-III-tubulin levels at day 10 of RA treatment (Figure 8B). pSUFU stably transfected knockout cells showed increased β-III-tubulin levels at day 14 of RA treatment compared to WT cells, which decreased by day 17 of treatment (Figure 8B), indicating that overexpressed *Sufu (*or *GLI3*) in *Sufu* knockout cells affects neuronal differentiation. To determine the effect this overexpression has on astrocyte differentiation, GFAP levels were explored following pSUFU or pGli3 stable transfection in *Sufu* knockout cells. Results showed no GFAP detection on day 10, but there was an increase by day 14 of RA treatment, albeit not to the levels observed in WT cells (Figure 8A and C). GFAP levels were maintained at day 17 in the pGli3 stably transfected cells, although pSUFU stably transfected cells had significantly decreased GFAP levels (Figure 8A and C). These differences seen with chicken *Sufu* overexpression were surprising, however, it may be the result of unexplored altered post-translational modifications to the chicken version of the protein. Nevertheless, these results show that chicken *Sufu* and human *GLI3* overexpression partially rescue astrocyte differentiation. This highlights not only the essential role of *Gli3* in neural differentiation, but a major role for SUFU to regulate GLI3 and produce the repressor form of this transcription factor.

## 4 Discussion

Hh signaling is involved in neural tube closure and neural differentiation *in vivo* [as reviewed by 1, 3] where the presence of Hh ligand induces a protein interaction cascade that results in the transcription of target genes through GLI transcription factors [3,7]. Negative regulators of the pathway include the transmembrane receptor Patched and the cytoplasmic regulator SUFU [3]. The loss of these essential regulators results in medulloblastoma and Nevoid Basal Cell Carcinoma Syndrome [12–14,27]; however, less is known about how the regulation of the pathway is involved in vertebrate neural cell fate determination. Using the mouse P19 embryonal carcinoma cell model we determined that early activation of Hh signaling is required for neural differentiation, but Hh activation alone is not sufficient to induce both neuron and astrocyte cell fates. Furthermore, SUFU was essential for *in vitro* neural differentiation as its loss activates Hh signaling through the loss of

the Gli3 transcription factor. This loss of SUFU resulted in the perturbed timing and proportion of differentiated astrocytes without affecting neuron differentiation. *Gli3* overexpression was sufficient

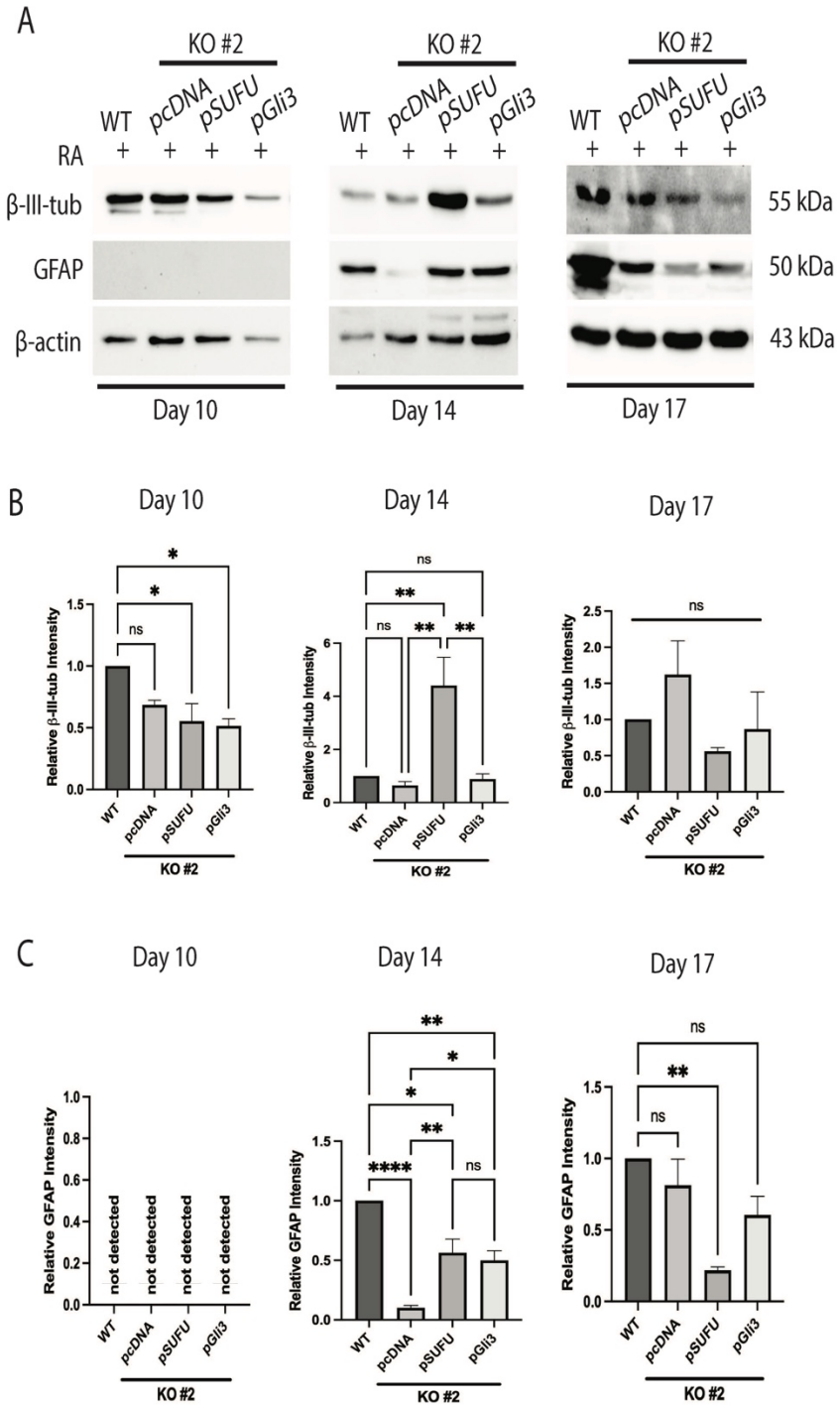


**Figure 8 –*Sufu* or *Gli3* overexpression partially rescues *Sufu*$^{-/-}$ phenotype. (A)** Immunoblot of neuron marker β-III-tubulin and astrocyte marker glial fibrillary acidic protein (GFAP) on days 10, 14 and 17 in *Sufu*$^{-/-}$ KO clone #2 cells transfected with pcDNA empty vector (pcDNA), or pcDNA-Chicken Sufu, or pcDNA-human Gli3 overexpression vectors and treated with RA. Densitometric analysis of **(B)** β-III-tubulin and **(C)** GFAP from the immunoblot in A. N=3. Bars represent mean values ± s.e.m. **P<0.05, **P<0.01, ****P<0.0001.*

to rescue the timing and proportion of astrocyte differentiation in SUFU deficient cells, pointing to it as downstream of the negative regulation imparted by SUFU. Moreover, this regulation is required to orchestrate the proper lineage determination of these neural cells.

### 4.1 Timing of Hh signaling

RA-induced neural differentiation of P19 cells is well established [18,19,28] where neurons are the predominant cell type after 10 days of treatment and subsequently decrease in numbers as immature and mature astrocytes proliferate [25], but few studies have explored Hh signaling in the model [20,21,29]. RA likely acts in these cells through the transcription factor FOXA1, which promotes the early expression of *Shh* [29], but the precise timing of pathway activation throughout differentiation has not been heretofore reported. We have shown that embryoid body formation with and without RA triggers Hh pathway activation early in neural specification and that the pathway is inactive during later stages of RA treatment (Figure 2). Although the mechanism of pathway activation in untreated cells remains unclear, these cells do not spontaneously differentiate towards neural lineages in the absence of RA (Figure 1E). Focusing on the RA-treated cells, like previous studies, we demonstrated that RA induced *Shh* expression, but *Ihh* and *Dhh* were also expressed (Figure 2). IHH and DHH, like SHH, can activate the pathway as evident in long bone differentiation [28, reviewed in 29] and gonad development [32–34], respectively. Similar results showing early transcriptional activation of all Hh ligands was reported with human embryonic stem cells induced to form neural tissues [35]. Thus, it is likely that SHH is responsible, but since transcripts encoding all ligands are induced by RA it remains unclear which isoform triggers pathway activation in the P19 model. Nevertheless, RA induction of a Hh ligand activates the pathway, and our evidence indicates that Hh signaling is attenuated during later stages of neural differentiation (Figure 2), coinciding with terminal neuron and astrocyte specification (Figure 1). Incidentally, previous Hh studies with P19 cells have only documented up to 8-10 days post RA-induction [20,29], where the present work investigates beyond terminal neuron differentiation. Although we, like others, have demonstrated the presence of Hh signaling in P19 neural differentiation, other signaling pathways including those linked to Wnt, Fgf and Yap are also involved during early P19 cell specification [21,36–38]. Considering our study, these other pathways require further investigation to determine if they too are temporally regulated to facilitate differentiation. However, since our focus was on Hh the importance of this pathway in neural differentiation was further investigated.

### 4.2 Early Hh activation is required but not sufficient to induce neural lineages

Utilization of RA to induce neural lineages *in vitro* goes beyond the P19 model, being consistently used for directed neural differentiation of human induced pluripotent stem cells and mouse embryonic stem cells [39,40]. Many neural differentiation protocols also supplement RA with exogenous SHH or SAG in order to enhance the differentiation of neurons [40–42] and glial cell progenitors [43]. Like these previous results, co-treating P19 cells with RA and SAG enhanced the differentiation of both neurons and astrocytes (Figure 3), although treating with SAG alone was not sufficient to induce differentiation. Unlike our work and the cited protocols, others have reported only an increase in neural progenitor proliferation and survival with SAG treatment with no change in neuron or glial cell numbers [44]; however this may be due to the lower concentrations used in this study. Despite these differences, we investigated the effect of inhibiting the Hh pathway using Cyc on neural differentiation. Inhibition of Hh signaling inhibited neuron and astrocyte differentiation (Figure 3), which is consistent with previous work showing Cyc co-treatment with RA decreased expression of neural-related transcription factors *Nkx2.2*, *Nkx6.1* and *Olig2* [42]. Thus, there is a requirement of early activation of Hh signaling in the differentiation of neural lineages, and we next

sought to understand the importance of later-stage inhibition of the Hh pathway by SUFU, its cytoplasmic negative regulator.

### 4.3 SUFU loss ectopically activates Hh target gene transcription

SUFU, a tumor suppressor protein required for mouse embryogenesis [10,12–14], must be regulated for Hh signaling to occur. A previous report shows that SUFU levels are depleted through the ubiquitin-proteasome pathway following Hh signal activation [45]. Hh ligand expression is induced within 1 day of RA treatment (Figure 2) and given previous reports on SUFU regulation, we had expected an early decrease in SUFU levels that might increase to basal levels later during differentiation. Our results, however, showed no significant change in SUFU levels during early neural differentiation, although there was a relative decrease later during astrocyte differentiation (Supplemental Figure 3). The mechanism of SUFU depletion at these later stages was not determined, nor were SUFU post-translational modifications examined at any stage, but it should be noted that differential phosphorylation and ubiquitination can both promote or inhibit SUFU stability and/or GLI interaction [46–49]. Instead of further examining post-translational modifications we used CRISPR-Cas9 and genetically depleted SUFU from P19 cells. CRISPR-Cas9-mediated knockout of *Sufu* supported previous *in vitro* studies in both mouse and human embryonic stem cells that show its loss induces the ectopic transcription of Hh target genes (Figure 4 and Figure 5) [14,35,50,51]. However, SUFU-deficient P19 cells did not differentiate in the absence of RA (Figure 6A) despite the previous report that *Gli2* overexpression in P19 cells was sufficient to induce neuron differentiation under similar conditions [20], or our work showing enhanced neural differentiation with SAG treatment (Figure 3).

### 4.4 SUFU loss causes loss of Gli3

Although we showed that the loss of SUFU ectopically activates the transcription of Hh target genes (Figure 4 and Figure 5) and this is well supported [14,35,50,51], the connection between aberrant astrocyte differentiation and SUFU deficiency came from examining Hh target genes later during the differentiation stages. At these stages *Gli1* and *Ptch1,* but not *Gli3*, expression was found to be higher when *Sufu* was knocked out (Figure 5). Previous reports with mouse show that SUFU is required for proper GLI3 processing [52] and its absence leads to reduced or absent GLI3 protein [11,50]. Conditional *Sufu* knockouts in the mouse brain also show reduced or absent GLI3 protein [15,16,53,54]. Together, our results support these studies showing the loss of GLI3 processing, and of GLI3 in general (Figure 5D) in the *Sufu* knock out cells is a reason to explain why there may be decreased and/or delayed astrocyte formation.

### 4.5 SUFU loss delays and decreases astrocyte differentiation

Since Hh signaling plays key roles during vertebrate brain development [55,56], the loss of SUFU or ectopic Hh signal activation is likely to affect neural differentiation. In support, when SUFU is knocked out in the mouse embryo the mutation is embryonic lethal and the resulting phenotypes mimic *Ptch1*$^{-/-}$ mutants [10,57]. Conditional knockouts of *Sufu* at various stages of brain development also results in decreased neuron differentiation and disorganized glial cell arrangements [15,53]. In human embryonic stem cells this knockout causes an increase in neuroectodermal gene expression following SHH treatment [35]. In contrast, however, no change is seen in ectoderm differentiation following *Sufu* knockout in mouse embryonic stem cells [51]. Discrepancies also exist within the same cell type as evident in P19 cells where *Gli2* overexpression induces neuron differentiation in the absence of RA [20], while *Gli2* knockdown produces the opposite effect [21]. Although the previous studies were done using different differentiation conditions, it is difficult to

explain these differences as our work showed the knockout of *Sufu* was accompanied by the consistent activation of Hh target gene expression (Figure 4 and Figure 5), but *Gli2* was not examined in *Sufu* KO lines. There was, however no detectable change in neuron differentiation in SUFU-deficient cells (Figure 6), which is in support of the work by Hoelzl et al. [51], who derived neuronal tissue from mouse embryonic stem cells depleted of SUFU. Moreover, our results showed a delay and decrease in astrocyte differentiation with the loss of SUFU (Figure 6 and Figure 7), which may explain the disorganization of glial cells observed in the conditional *Sufu* knockouts described in mouse embryos [15,53]. Overall, our research indicates that Hh signaling is induced by RA, but the pathway must remain in the *off* state for proper astrocyte differentiation. Given that glial cell populations are composed of astrocytes, oligodendrocytes and microglia further research must be done to explore the effect of SUFU loss on these other glial-cell lineages.

### 4.6 Gli3 overexpression rescues Sufu knockout phenotype

We showed that there was a loss of GLI3 in the SUFU-deficient cells (Figure 5) and provide evidence that ectopic expression of GLI3 was sufficient to rescue the timing of glial cell differentiation in these cells (Figure 8). That *GLI3* was able to rescue the *Sufu* knockout phenotype is supported by previous research where overexpression of the *Gli3* repressor in Sufu-deficient mouse cerebellums was sufficient to rescue morphology and increase GFAP levels [16]. Together, our results clearly show that SUFU imparts its negative regulation on the Hh pathway by acting on Gli3 and this transcription factor is required later during the specification of neural cells into neurons and astrocytes.

### 4.7 Conclusion

We have reported the Hh signaling profile in P19 neurogenesis, have shown a required role of early pathway activation and demonstrated an essential role of a negative regulator of this pathway, SUFU, in maintaining the pathway in the off state to allow proper astrocyte differentiation. We propose that the mechanism of astrocyte differentiation requires SUFU, however given our rescue studies SUFU is required to maintain appropriate Gli3 levels, which are required for astrocyte determination.

## 5 Conflict of Interest

*The authors declare that the research was conducted in the absence of any commercial or financial relationships that could be construed as a potential conflict of interest.*

## 6 Author Contributions

Conceptualization, D.M.S. and G.M.K.; methodology, D.M.S.; flow cytometry analysis, J.G.D.; formal analysis, G.M.K. and D.M.S.; writing, first draft—D.M.S.; writing—review and editing, D.M.S. and G.M.K.; supervision, G.M.K.; funding acquisition, G.M.K. All authors have read and agreed to the published version of the manuscript.

## 7 Funding

This research was funded by the Natural Sciences and Engineering Research Council (NSERC) of Canada, Discovery Grant R2615A02 to G.M.K. D.M.S. acknowledges support from the School of Graduate and Postdoctoral Studies, University of Western Ontario; the Collaborative Graduate Specialization in Developmental Biology, University of Western Ontario; the Children's Health Research Institute; and NSERC for a PGS D scholarship.

## 8 Acknowledgments

We would like to thank members past and present of the Kelly lab for helpful discussions.

## 9 References

1. Wilson L and M Maden (2005). The mechanisms of dorsoventral patterning in the vertebrate neural tube. Dev Biol 282: 1–13.
2. Dahmane N and A Ruiz (1999). Sonic hedgehog and cerebellum development. Development 3100: 3089–3100.
3. Briscoe J and PP Thérond (2013). The mechanisms of Hedgehog signalling and its roles in development and disease. Nat Rev Mol Cell Biol 14: 418–431.
4. Han Y, Q Shi and J Jiang (2015). Multisite interaction with Sufu regulates Ci/Gli activity through distinct mechanisms in Hh signal transduction. Proc Natl Acad Sci 112: 6383–6388.
5. Tempe D, M Casas, S Karaz, M-F Blanchet-Tournier and J-P Concordet (2006). Multisite Protein Kinase A and Glycogen Synthase Kinase 3 Phosphorylation Leads to Gli3 Ubiquitination by SCF TrCP. Mol Cell Biol 26: 4316–4326.
6. Hui C and S Angers (2011). Gli proteins in development and disease. Annu Rev Cell Dev Biol 27: 513–537.
7. Humke EW, K V. Dorn, L Milenkovic, MP Scott and R Rohatgi (2010). The output of Hedgehog signaling is controlled by the dynamic association between Suppressor of Fused and the Gli proteins. Genes Dev 24: 670–682.
8. Haycraft CJ, B Banizs, Y Aydin-Son, Q Zhang, EJ Michaud and BK Yoder (2005). Gli2 and Gli3 localize to cilia and require the intraflagellar transport protein Polaris for processing and function. PLoS Genet 1: e53.
9. Svärd J, KH Henricson, M Persson-Lek, B Rozell, M Lauth, Å Bergström, J Ericson, R Toftgård and S Teglund (2006). Genetic elimination of suppressor of fused reveals an essential repressor function in the mammalian hedgehog signaling pathway. Dev Cell 10: 187–197.
10. Cooper AF, KP Yu, M Brueckner, LL Brailey, L Johnson, JM McGrath and AE Bale (2005). Cardiac and CNS defects in a mouse with targeted disruption of suppressor of fused. Development 132: 4407–4417.
11. Makino S, O Zhulyn, R Mo, V Puviindran, X Zhang, T Murata, R Fukumura, Y Ishitsuka, H Kotaki, D Matsumaru, S Ishii, CC Hui and Y Gondo (2015). T396I mutation of mouse Sufu reduces the stability and activity of Gli3 repressor. PLoS One 10: 1–15.
12. Taylor MD, L Liu, C Raffel, C chung Hui, TG Mainprize, X Zhang, R Agatep, S Chiappa, L Gao, A Lowrance, A Hao, AM Goldstein, T Stavrou, SW Scherer, WT Dura, B Wainwright, JA Squire, JT Rutka and D Hogg (2002). Mutations in SUFU predispose to medulloblastoma. Nat Genet 31: 306–310.
13. Smith MJ, C Beetz, SG Williams, SS Bhaskar, JO Sullivan, B Anderson, SB Daly, JE Urquhart, Z Bholah, D Oudit, E Cheesman, A Kelsey, MG Mccabe, WG Newman, DGR Evans, MJ Smith, SG Williams, E Urquhart, Z Bholah and G William (2018). Germline mutations in SUFU cause Gorlin Syndrome – Associated Childhood Medulloblastoma and redefine the risk associated with PTCH1 mutations. J Clin Oncol 32: 4155–4161.
14. Urman NM, A Mirza, SX Atwood, RJ Whitson, KY Sarin, JY Tang and AE Oro (2016). Tumor-derived suppressor of fused mutations reveal hedgehog pathway interactions. PLoS One 11: 1–10.
15. Kim JJ, T Jiwani, S Erwood, J Loree and ND Rosenblum (2018). Suppressor of fused controls cerebellar neuronal differentiation in a manner modulated by GLI3 repressor and Fgf15. Dev Dyn 247: 156–169.
16. Kim JJ, PS Gill, L Rotin, M van Eede, RM Henkelman, C-C Hui and ND Rosenblum (2011).

Suppressor of Fused controls mid-hindbrain patterning and cerebellar morphogenesis via GLI3 repressor. J Neurosci 31: 1825–1836.
17. Mcburney M (1993). P19 embryonal carcinoma cells. Int J Dev Biol 37: 135–140.
18. McBurney MW, EMV Jones-Villeneuve, MKS Edwards and PJ Anderson (1982). Control of muscle and neuronal differentiation in a cultured embryonal carcinoma cell line. Nature 299: 165–167.
19. McBurney MW, KR Reuhl, a I Ally, S Nasipuri, JC Bell and J Craig (1988). Differentiation and maturation of embryonal carcinoma-derived neurons in cell culture. J Neurosci 8: 1063–1073.
20. Voronova A, A Fischer, T Ryan, A Al Madhoun and IS Skerjanc (2011). Ascl1/Mash1 is a novel target of Gli2 during Gli2-induced neurogenesis in P19 EC cells. PLoS One 6:.
21. Lin YT, JY Ding, MY Li, TS Yeh, TW Wang and JY Yu (2012). YAP regulates neuronal differentiation through Sonic hedgehog signaling pathway. Exp Cell Res 318: 1877–1888.
22. Ran FA, PD Hsu, J Wright, V Agarwala, DA Scott and F Zhang (2013). Genome engineering using CRISPR-Cas9 system. Nat Protoc 8: 2281–2308.
23. Brinkman EK, T Chen, M Amendola and B Van Steensel (2014). Easy quantitative assessment of genome editing by sequence trace decomposition. Nucleic Acids Res 42: 1–8.
24. Pearse R V., LS Collier, MP Scott and CJ Tabin (1999). Vertebrate homologs of Drosophila Suppressor of fused interact with the Gli family of transcriptional regulators. Dev Biol 212: 323–336.
25. McBurney M (1993). P19 embryonal carcinoma cells. Int J Dev Biol 140: 135–140.
26. Dunaeva M, P Michelson, P Kogerman and R Toftgard (2003). Characterization of the physical interaction of Gli proteins with SUFU proteins. J Biol Chem 278: 5116–5122.
27. Hahn H, C Wicking, PG Zaphiropoulos, MR Gailani, S Shanley, A Chidambaram, I Vorechovsky, E Holmberg, AB Unden, S Gillies, K Negus, I Smyth, C Pressman, DJ Leffell, B Gerrard, AM Goldstein, M Dean, R Toftgard, G Chenevix-Trench, B Wainwright and AE Bale (1996). Mutations of the human homolog of drosophila patched in the nevoid basal cell carcinoma syndrome. Cell 85: 841–851.
28. Jones-Villeneuve EM, MW McBurney, KA Rogers and VI Kalnins (1982). Retinoic acid induces embryonal carcinoma cells to differentiate into neurons and glial cells. J Cell Biol 94: 253–262.
29. Tan Y, Z Xie, M Ding, Z Wang, Q Yu, L Meng, H Zhu, X Huang, L Yu, X Meng and Y Chen (2010). Increased levels of FoxA1 transcription factor in pluripotent P19 embryonal carcinoma cells stimulate neural differentiation. Stem Cells Dev 19: 1365–1374.
30. St-Jacques B, M Hammerschmidt and AP McMahon (1999). Indian hedgehog signaling regulates proliferation and differentiation of chondrocytes and is essential for bone formation. Genes Dev 13: 2072–2086.
31. Bechtold TE, E Koyama, N Kurio, HD Nah, C Saunders and PC Billings (2019). The roles of Indian hedgehog signaling in TMJ formation. Int J Mol Sci 20:.
32. Bashamboo A and K McElreavey (2015). Human sex-determination and disorders of sex-development (DSD). Semin Cell Dev Biol 45: 77–83.
33. Bitgood MJ, L Shen and AP McMahon (1996). Sertoli cell signaling by Desert hedgehog regulates the male germline. Curr Biol 6: 298–304.
34. Clark AM, KK Garland and LD Russell (2000). Desert hedgehog (Dhh) gene is required in the mouse testis for formation of adult-type Leydig cells and normal development of peritubular cells and seminiferous tubules. Biol Reprod 63: 1825–1838.
35. Wu SM, ABH Choo, MGS Yap and KKK Chan (2010). Role of Sonic hedgehog signaling and the expression of its components in human embryonic stem cells. Stem Cell Res 4: 38–49.
36. Tang K, J Yang, X Gao, C Wang, L Liu, H Kitani, T Atsumi and N Jing (2002). Wnt-1 promotes neuronal differentiation and inhibits gliogenesis in P19 cells. Biochem Biophys Res Commun 293: 167–173.

37. Jing XT, HT Wu, Y Wu, X Ma, SH Liu, YR Wu, XF Ding, XZ Peng, BQ Qiang, JG Yuan, WH Fan and M Fan (2009). DIXDC1 promotes retinoic acid-induced neuronal differentiation and inhibits gliogenesis in P19 cells. Cell Mol Neurobiol 29: 55–67.
38. Chen W, X Caihong, B Wei, L Li, W Lin, Y-G Chen, S-L Ang and N Jing (2006). Cell aggregation-induced FGF8 elevation Is essential for P19 cell neural differentiation. Mol Biol Cell 17: 3075–3084.
39. Fraichard A, O Chassande, G Bilbaut, C Dehy, P Savatier and J Samarut (1995). In vitro differentiation of embryonic stem cells into glia and neutrons. J Cell Sci 108: 3181–3188.
40. Mak SK, YA Huang, S Iranmanesh, M Vangipuram, R Sundararajan, L Nguyen, JW Langston and B Schüle (2012). Small molecules greatly improve conversion of human-induced pluripotent stem cells to the neuronal lineage. Stem Cells Int 2012:.
41. Wu CY, D Whye, RW Mason and W Wang (2012). Efficient differentiation of mouse embryonic stem cells into motor neurons. J Vis Exp 1–5.
42. Okada Y, T Shimazaki, G Sobue and H Okano (2004). Retinoic-acid-concentration-dependent acquisition of neural cell identity during in vitro differentiation of mouse embryonic stem cells. Dev Biol 275: 124–142.
43. Li S, J Zheng, L Chai, M Lin, R Zeng, J Lu and J Bian (2019). Rapid and Efficient Differentiation of Rodent Neural Stem Cells into Oligodendrocyte Progenitor Cells. Dev Neurosci 41: 79–93.
44. Bragina O, S Sergejeva, M Serg, T Žarkovsky, A Maloverjan, P Kogerman and A Žarkovsky (2010). Smoothened agonist augments proliferation and survival of neural cells. Neurosci Lett 482: 81–85.
45. Yue S, Y Chen and SY Cheng (2009). Hedgehog signaling promotes the degradation of tumor suppressor Sufu through the ubiquitin-proteasome pathway. Oncogene 28: 492–499.
46. Takenaka K, Y Kise and H Miki (2007). GSK3β positively regulates Hedgehog signaling through Sufu in mammalian cells. Biochem Biophys Res Commun 353: 501–508.
47. Infante P, R Faedda, F Bernardi, F Bufalieri, LL Severini, R Alfonsi, D Mazzà, M Siler, S Coni, A Po, M Petroni, E Ferretti, M Mori, E De Smaele, G Canettieri, C Capalbo, M Maroder, I Screpanti, M Kool, SM Pfister, D Guardavaccaro, A Gulino and L Di Marcotullio (2018). Itch/β-Arrestin2-dependent non-proteolytic ubiquitylation of SuFu controls Hedgehog signalling and medulloblastoma tumorigenesis. Nat Commun 9: 1–17.
48. Chen Y, S Yue, L Xie, XH Pu, T Jin and SY Cheng (2011). Dual phosphorylation of suppressor of fused (Sufu) by PKA and GSK3β regulates its stability and localization in the primary cilium. J Biol Chem 286: 13502–13511.
49. Wang Y, Y Li, G Hu, X Huang, H Rao, X Xiong, Z Luo, Q Lu and S Luo (2016). Nek2A phosphorylates and stabilizes SuFu: A new strategy of Gli2/Hedgehog signaling regulatory mechanism. Cell Signal 28: 1304–1313.
50. Chen MH, CW Wilson, YJ Li, KK Lo Law, CS Lu, R Gacayan, X Zhang, CC Hui and PT Chuang (2009). Cilium-independent regulation of Gli protein function by Sufu in Hedgehog signaling is evolutionarily conserved. Genes Dev 23: 1910–1928.
51. Hoelzl MA, K Heby-Henricson, G Bilousova, B Rozell, R V Kuiper, M Kasper, R Toftgård and S Teglund (2015). Suppressor of Fused plays an important role in regulating mesodermal differentiation of murine embryonic stem cells In vivo. Stem Cells Dev 24: 2547–2560.
52. Kise Y, A Morinaka, S Teglund and H Miki (2009). Sufu recruits GSK3β for efficient processing of Gli3. Biochem Biophys Res Commun 387: 569–574.
53. Yabut OR, G Fernandez, K Yoon, SJ Pleasure, OR Yabut, G Fernandez, T Huynh, K Yoon and SJ Pleasure (2015). Suppressor of Fused Is critical for maintenance of neuronal progenitor identity during corticogenesis. Cell Rep 12: 2021–2034.
54. Jiwani T, JJ Kim and ND Rosenblum (2020). Suppressor of fused controls cerebellum granule

cell proliferation by suppressing Fgf8 and spatially regulating Gli proteins. Development 147: 1–17.
55. Memi F, N Zecevic and N Radonjić (2018). Multiple roles of Sonic Hedgehog in the developing human cortex are suggested by its widespread distribution. Brain Struct Funct 223: 2361–2375.
56. Belgacem YH, AM Hamilton, S Shim, KA Spencer and LN Borodinsky (2016). The many hats of Sonic hedgehog signaling in nervous system development and disease. J Dev Biol 4:.
57. Goodrich L V., L Milenković, KM Higgins and MP Scott (1997). Altered neural cell fates and medulloblastoma in mouse patched mutants. Science (80- ) 277: 1109–1113.